Granular Matter
DOI 10.1007/s10035-010-0202-y

Ant tunneling—a granular media perspective

D. Nicolas Espinoza · J. Carlos Santamarina

Received: 1 July 2009

Abstract Laboratory and field data show that the digging habits of ants and the resulting nest architecture vary with soil conditions, yet, the geomechanical understanding of ant tunneling is lacking. We study the excavation strategies used by harvester ants in clay, silt, sand, and gravel at water contents that range from dry to saturated. The study focuses on the conditions at the tunnel face that determine particle removal methods, digging rate, the development of branches, and tunneling patterns. Analytical and numerical models provide particle-level insight into the experimental observations and help identify the causal links that relate ants digging performance and nest geometric patterns with the properties of the granular medium such as grain size, moisture, and packing density. Results highlight ants' exceptional ability to sense the prevailing geomechanical conditions in tunnels, and to adapt excavation strategies, transport methods and tunneling patterns to those conditions, within their inherent size and strength limitations. The resulting tunnel structure emerges as a mechanically-convenient and energy-efficient topology based on local information gather by ants along the tunnel and at the tunnel face.

Keywords Ant nest · Tunnel stability · Digging · Micromechanics · Discrete element method

D. N. Espinoza (✉) · J. C. Santamarina
School of Civil and Environmental Engineering,
Georgia Institute of Technology, Atlanta, GA, USA
e-mail: nicolas@ce.gatech.edu
URL: http://pmrl.ce.gatech.edu

J. C. Santamarina
e-mail: jcs@gatech.edu
URL: http://pmrl.ce.gatech.edu

1 Introduction

Evolution has lead to adaptable, multifunctional, self-healing and recyclable organisms [1]. Biomimesis seeks to understand nature's design and to imitate it in renewed and enhanced engineering concepts for the built environment. In this study we consider ants because of their unique and efficient tunnel excavation abilities in granular media. Ants adapt to a wide range of soils. They are found in fine grained soils with high clay content [2–10], silty soils and loess (P. occidentalis, [9]), sands [2,5,6,9,11–16], and even gravels [9,17,18]. In fact, different soils are often found in the same nest [9,19], implying adaptable nest construction capabilities. Physical as well as chemical properties of the soil may be altered in nests [20].

Harvester ants, including the genera *Pogonomyrmex* ("P." here on) develop large underground nests. Their activity and distribution depend on biotic as well as abiotic factors such as parasites, predators, vegetation, porewater salinity, soil moisture and grain size [5]. Water affects all aspects of harvester ants' behavior [5,8,13]. They prefer wet and sun-covered areas [6,8,9,21,22]. Eventually, lack of water leads to desiccation and death; therefore, ant counts correlate with precipitation and soil characteristics that affect water retention [5]. Harvester ants may live comfortably in arid and semiarid environments; the water content in the nest soil can range between 4 and 20%. Water saturation often causes tunnel collapse and limits nest depth [9]. Soil temperature affects digging behavior as well [23].

The spatial arrangement and configuration of tunnels and chambers are similar for many ant species [11,24]; the morphology of the nest may be linked to the number of queens in the nest as well [22]. Most nests consist of major vertical shafts which link vertically flattened horizontal chambers [11,25].

Published online: 10 September 2010

Nests are built by soil removal rather than soil piling [11] and most species follow the same grab-rake-transport sequence [13,26,27]. The preferred particle size depends on the mandible size, and they can handle particles as large as their head (some species of *P. genera* successfully transport particles between 2 and 5 mm in size, [9,10,17,28]). Tunnel stability may be enhanced by glandular secretion ([8], similar to some termite species, [29]), ants dejection [9,30], and natural soil cementation.

The previous observations underscore the importance of soil type and moisture on the digging and nesting behavior of ants. The purpose of this study is to identify the fundamental geomechanical principles and granular media properties that determine digging methods and nest geometric patterns.

2 Methods

The experimental study was designed to discern the geomechanical phenomena that determine the digging behavior of ants at the tunnel face, and its effect on nest architecture. Therefore, while we monitor the whole network, we focus our attention on the activity of individual ants at the tunnel face (see field studies in [11,24]).

2.1 Ants

We selected harvester ants genera *Pogonomyrmex barbatus* because of their prolific digging behavior (supplier: Carolina Biological and Life Studies). They are ~8 mm long, the side-to-side leg contact width is about 7 mm, the mandible can open ~2 mm wide and their average weight is 9×10^{-5} N. No queens are used in this study.

2.2 Sediments

The six natural granular media used for these tests are (see Table 1): Crushed granite gravels CG 6/10 (mean size $d_{50} =$ 3,000 μm) and CG 10/14 ($d_{50} = 1{,}900$ μm), Ottawa sand OS 20/30 ($d_{50} = 730\ \mu$m), Fine sand F110 ($d_{50} = 110$ μm),

Table 1 Experimental study. Soil characteristics and tunnel size

Soil properties				Water content					Ant	Tunnel size		
Material	d_{50} [μm]	Particle shape	ρ_{dry} [g/cm^3]	Saturation S [%]					M/d_{50}	D_{min} [cm]	D_{max} [cm]	D_{mean}/d_{50}
Gravel CG 6/10	3,000	Angular	1.40	0					0.7	0.5	0.6	2.7
			1.24		11	35						
			1.10		11							
Gravel CG 10/14	1,900	Angular	1.24	0	11				1.1	0.5	1	3.7
			1.10		11							
Sand OS 20/30	730	Rounded	1.90	0					2.7	0.4	1	8
			1.80	0								
			1.75	0								
			1.67		20	40	60					
			1.52		20	40	60					
Sand F110	110	Sub-rounded	1.65					93	13.3	0.3	0.9	>35
			1.58	0								
			1.40	0	12	24	36					
			1.10		12	24	36					
Silt SF	5	Angular	1.50					95	400	0.3	1.2	>1000
			1.39	0								
			1.12	0								
			0.90		7	13	20					
			0.70		7	13	20					
Clay KC	0.4	Platy	1.2	0					>5,000	0.5	0.5	>15000

Note: The coefficient of uniformity $C_u = d_{60}/d_{10}$ for gravels and sands is $C_u < 1.7$ and it is $C_u \sim 10$. for silt and clay
Abbreviations: Crushed granite CG (CG 6/10: pass sieve #6 and retained in #10. CG 10/14: pass sieve #10 and retained in #14). Ottawa sand OS. Fine sand F110 (mean grain size 110 μm). Crushed silica flour SF. Kaolinite clay KC
Notation: Dry bulk density ρ_{dry}. Water saturation S. Mandible size M. Tunnel diameter D. Mean grain size d_{50}

Silica flour silt SF ($d_{50} = 5$ μm), and Kaolinite clay KC ($d_{50} = 0.4$ μm). Soil beds are formed with different water contents ω and compaction densities. All together, the investigation involves 39 experiments as summarized in Table 1. Each experiment starts with a fresh set of ants.

2.3 Procedure

Narrow transparent rectangular acrylic boxes are used to house the soil beds (18.2 cm length, 10.6 cm height and 1.25 cm width). The selected soil is compacted at the target water content ω in layers parallel to the bottom boundary. The box is kept at room temperature under laboratory illumination (see implications in [23,25,27]). Holes through the upper rigid boundary give ants access to the soil. A group of 10–20 ants is introduced in each box; they are fed once a week and water is supplied to the ants regularly (we attempt to maintain the soil moisture constant).

2.4 Monitoring

Ants' movement, general digging strategies and detailed information about face excavation are gathered by continuous visual observation and through high resolution time-lapse digital photography. Therefore, tunnel width, length and direction can be determined at all times.

3 Results

The most important qualitative observations and quantitative measurements gathered in this study are summarized next. Additional observations can be found in Table 2.

3.1 Excavation process

The excavation sequence follows: 1- evaluation of local conditions using antennae as particle-level sensors to asses particle mobility; 2-particle removal using mandibles or material gathering with legs; 3-transportation of the load held with mandibles; and 4-return to the tunnel face. This sequence agrees with published studies [13,26].

3.2 Particle removal

The different approaches used to remove particles at the tunnel face vary with grain size d relative to mandible size M and water content ω (Fig. 1). In the case of fine silts and clayey soils, ants remove the soil and form loose particle conglomerates when the water content is very low; as the

Table 2 Tunnel characteristics—additional observations (see Fig. 3)

Fine grained	KC	Tunneling is limited under most moisture conditions, and it is restricted to the upper boundary when the water content is near saturation Tunnel paths are curved, there are no intersections or branches, and all tunnels are about the same size
	SF	Tunnels are smooth and follow curved paths, even closed loops. Excavation is limited to the upper boundary when the water content is near saturation. Shafts are not common There are frequent incipient branches when the soil is packed at low density. Intersections are not common The tunnel diameter is highly variable, particularly at low soil density. The largest tunnels and the shortest separation between parallel tunnels are observed at intermediate saturation. Big cavities are frequently observed
Coarse grained	F110	Tunnels are excavated at any angle, yet, most of them are inclined at 30-to-45°; there are a few short vertical shafts. The longest straight tunnels are observed when the sand is dense Branching is most common at low water content. Intersections are scarce; the largest intersections are built at intermediate saturation and low soil density There is significant variability in tunnel diameter
	OS 20/30	Most tunnels are excavated along straight paths and inclined at 45° or less. Curved and smooth tunnels are most common at high water content and low soil density Branches are common and they are aligned normal to the direction of the main tunnel. Intersections with preexisting tunnels are common as well All tunnels are about the same size D, and there is no enlargement at intersections
	CG 6/10 10/14	Excavation starts by digging a vertical shaft downwards until the lower boundary is encountered. Then, other shafts are excavated upwards. There are some convoluted and irregular, small size "passages" between grains (rather than excavated tunnels) Most tunnels are along straight paths. Some irregular tunnels paths are observed in the more densely packed gravels. Tunnel diameters are uniform throughout the network There are no branches or intersections, and the separation between tunnels is large Collapses during excavation are frequent, even in moist gravel

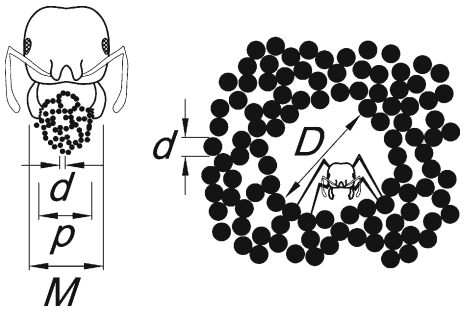

Fig. 1 Geometric characteristics—size definition: ant mandible size M, soil grain size d, pellet size p and tunnel diameter D

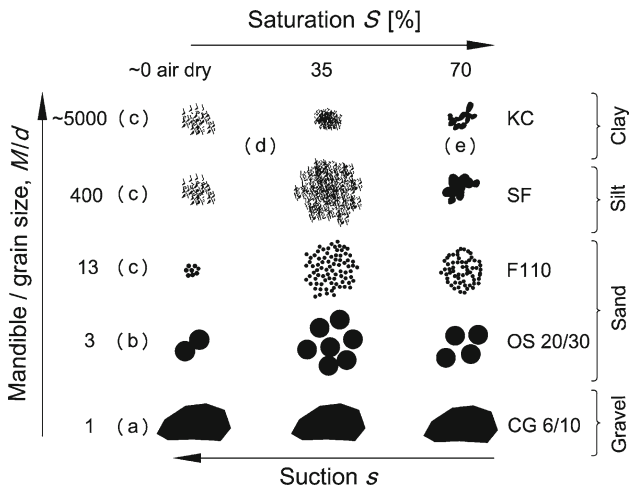

Fig. 2 Particle removal strategies as a function of relative mandible-to-grain size M/d and capillary forces in terms of water saturation $S\%$ or suction s. **a** Single grain. **b** Few grains held by friction, augmented by capillary effects. **c** Capillarity is critical for the effective excavation and transport of multiple particles. **d** Loose conglomerates formed by raking with legs. **e** High attractive forces limit excavation to small blocks followed by pellet formation for effective transport

water content increases, particle removal in fine soils consists of successive grabs that are grouped to form bigger and more stable pellets (Fig. 2). Wet pellets can reach $p \approx 3$ mm in diameter. Cutting blocks with mandibles is a strategy used in clays and silts near saturation.

Ants can successfully grab several dry sand particles at once: the transport of dry coarse soils is limited by the maximum number of particles that can be grabbed and held by friction; our observations show three particles for sand OS 20/30 and a maximum of 13 particles for the finer F110 sand. Yet, a more stable sand pellet is formed when water is present. Ants use their beard to facilitate the transportation of both sandy and silty sediments.

As particle size increases and reaches gravel size, e.g. CG 6/10, excavation consists of single particle removal regardless of the water content. Ants choose particles by size and identify the smallest section to grab them so that the width does not exceed the mandible size (see similar observation with P. occidentalis in Ref. [9]).

3.3 Tunnel patterns

Figure 3 shows sketches of observed excavation patterns as a function of degree of saturation and grain size. Tunnels parallel to the transparent wall are of regular thickness and height, and those that depart from the wall are nearly circular. The limited dimensions of the nest boxes do not allow flattened tunnels or chambers.

Excavation in fine-grained clay KC is limited to short tunnels near the upper boundary of the sediments. On the other hand, a widespread tunnel network in all directions is observed in silt SF at low-to-medium water content. Excavation in dry sands, F110 and OS 20/30, causes granular sliding, therefore ants transform level-ground into a sand pile at the angle of repose. Yet, moist sands are stable at the tunnel scale and can support extensive tunnel networks.

Excavation in dry fine gravel CG 10/14 is prone to granular sliding, as in sands. Occasional short and intricate small size "passages" can be seen in the coarser CG 6/10 gravel; tunnels size $D >\sim 6$ mm are built occasionally in moist gravels. In all cases, particle removal in these coarse soils takes place from the base of shafts or even the top face in upwards excavation rather than lateral grabs from walls. Therefore, vertical shafts are more frequent than horizontal tunnels. Instability always threatens particle excavation in both dry and moist gravels, and tunnel collapse often leads to ants becoming trapped.

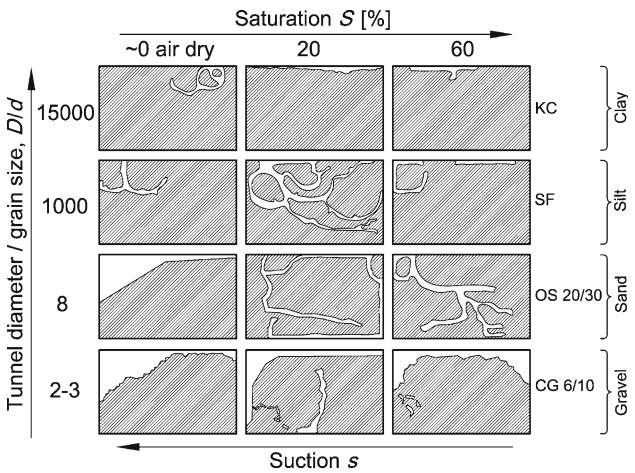

Fig. 3 Tunneling patterns as a function of grain size and capillary forces in terms of water saturation $S\%$ or suction s—harvester ants under laboratory conditions. Ants start digging on the top boundary. Experiments in fine sand F110 present similar features to those in silt SF at intermediate saturations. Particle sliding dominates in air-dry sands and gravels. Boundary conditions limit tunnel topologies to a narrow region—we anticipate richer tunnel topologies in 3D settings

3.4 Direction, branches and intersections

Tunnel direction is strongly affected by interfaces between different materials. In fact, initial tunnels are typically built against rigid boundaries such as the frame of the lab nest. Salient geometric characteristics for tunnels in different soils are summarized in Table 2.

Tunnel branches and intersections are common when soil conditions and water contents allow for stable tunnels. Intersections develop when an advancing tunnel encounters a pre-existing one; intersections are more common in sands. Branches result from 'lateral grabs' from tunnel walls; main branches and multiple incipient yet not fully developed branches are seen in silts and sands. For a given soil, the relative quantity of branches increases as the packing density of the sediment decreases. There are few major branches and no incipient branches in the moist gravel CG 10/14; no branches are observed in the coarse gravel CG 6/10 and in fine soils with high saturation.

3.5 Size

The average tunnel size is relatively constant and it ranges from $D = 5$-to-6 mm in all tested soils, regardless of grain size or moisture condition. The excavated space is larger at tunnel intersections, particularly in moist silts and fine sands (details in Table 2).

3.6 Digging rates

Digging rates vary between 0.02-and-2 $\mathrm{cm^3 day^{-1} ant^{-1}}$. The fastest digging rates are attained in slightly wet sands (F110, $d_{50} = 100\,\mu$ m, water saturation $S \approx 15\%$), and the lowest ones in fine-grained clay KC and coarse gravels CG. Digging rates inferred from published studies in natural sandy nests range from 0.1-to-1 $\mathrm{cm^3\ day^{-1}\ ant^{-1}}$ (based on observations in [11,25]).

4 Analysis and discussion

The new experimental results reported above corroborate previous field and laboratory observations and provide unprecedented information related to the interplay between grain size and water content. In this section we seek physical and geomechanical explanations to the observed digging behavior of ants, with emphasis on single-ant response at the tunnel face.

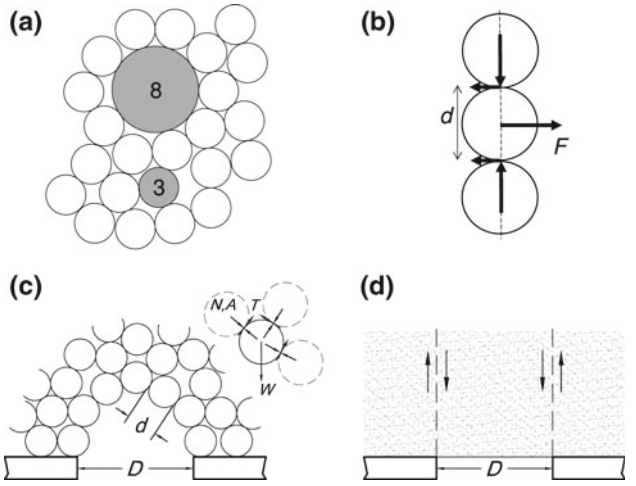

Fig. 4 Geomechanical mechanisms: **a** Coordination number *CN*. A large particle has a higher coordination number than a smaller one. The *numbers* shown correspond to this 2D example. **b** Pull-force F required to remove a load-bearing particle size d from a granular chain. **c** Tunnel stability analysis: Particle-level analysis for large grains when $D/d <\sim 15$; and **d** equivalent continuum material model and kinematically admissible failure mode for situations when $D/d >> 1$

4.1 Geometric constraints

4.1.1 Mandible to particle size M/d

The relative mandible-to-particle size becomes the limiting factor for particle removal in coarse gravels as the ratio approaches to $M/d \approx 1$ (see Fig. 1). When particles are $d < M$, ants prefer to grab smaller single particles in a gravel pack even though grabbing and transporting the largest possible particle would appear more energetically efficient. The geomechanical explanation is based on the average number of contacts per particle or coordination number *CN* (Fig. 4-a). The coordination number of a boundary particle in a random packing of monosized particles varies from 3-to-5. In a packing of bimodal-size particles, small boundary particles d_{small} still have $CN = 3$-to-5, but big boundary particles d_{large} have a number of contacts proportional to $\sim \pi/2\ (d_{large}/d_{small})^2$ based on the ratio of the big particle surface area to the equatorial area of the small particles [see numerical simulations in Ref. 31]. Thus, the high coordination of large particles hinders its removal.

Digging rates in dry coarse soils are limited by the ants' ability to hold more than one particle together by friction, therefore, digging rates improve as M/d decreases in dry coarse soils.

4.1.2 Mandible to pellet size M/p

Transport is based on pellets when the mandible size M is considerable greater than the particle size d, such as in clay

KC ($M/d \approx 5{,}000$) and silt SF ($M/d \approx 400$), as shown in Fig. 2. Moisture helps form stable pellets in sands as well. The measured size of pellets p is related to mandible size in all cases: M/p =1/2-to-2. Higher digging rates are observed when larger pellets can be formed.

4.1.3 Tunnel diameter to ant height D/H

The tunnel characteristic size D is primarily linked to trafficability and the ability of ants to walk-pass each other (see Fig. 1). Harvester ants used in this study rise $H = 3$ mm above a horizontal plane and most tunnels are $D \geq 6$ mm, so that $D \geq 2H$. In agreement with trafficability needs, published data show that nests with thousands of ants can have a shaft diameter $D = 20$ mm close to the surface where traffic is greatest, decreasing to around 10 mm in deeper sections (P. badius with similar height, [11]).

4.2 Particle-level force analysis

Capillary and electrical interparticle forces play a major role on ant tunneling as they affect face stability conditions as well as pelletization and transport. The following particle-level analysis considers spherical particles of diameter d and compares interparticle capillary forces C in the pendular regime, van der Waals electrical attraction A_{elec}, the self weight of particles $W$and the pulling force of ants mandible U.

4.2.1 Capillary force C

The capillary force $C = a_m s$ between two spherical particles is determined by the cross sectional area of the water meniscus at interparticle contacts a_m and the suction in the water $s = -(u_a - u_w)$ which is the difference between the air u_a and water u_w pressures. Furthermore, we can relate suction s to the water content ω in the soil and the air-water surface tension $\sigma = 73$ mN/m through Laplace's equation leading to the following expression [32],

$$C = a_m s = \frac{\pi}{2}\sigma d\left[2 - \left(\frac{8}{9}\omega G_S\right)^{1/4}\right] \tag{1}$$

where G_S is the specific gravity of the mineral.

4.2.2 Electrical force E

The electrical van der Waals attractive force E depends on the Hamaker constant A_h ($A_h = 0.83 \times 10^{-20}$ J for quartz-water-quartz) and the inter-particle separation t between the two spherical particles size d (see details in [33]),

$$E = \frac{A_h}{24t^2}d \tag{2}$$

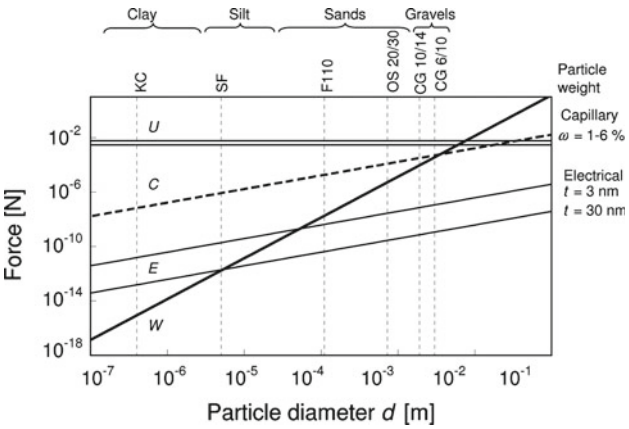

Fig. 5 Interparticle forces as a function of particle size. Capillary forces are computed in the pendular regime, i.e. low water content. Assumed parameters: mineral specific gravity $G_S = 2.65$, surface tension $\sigma = 73$ mN/m, Hamaker constant $A_h = 0.83 \times 10^{-20}$J. The slopes of lines in this log–log plot are 3 for particle weight $W = f(d^3)$ and 2 for electrical and capillary forces as they are proportional to d^2

4.2.3 Particle weight W

The weight of a spherical particle size d made of a mineral of specific gravity G_S is

$$W = \frac{\pi}{6}d^3 G_S g \rho_w \tag{3}$$

where gravity is $g = 9.81$ m/s^2 and the mass density of water is $\rho_w = 1{,}000$ kg/m^3.

4.2.4 Ant pulling force U

The pulling force ants can exert with their mandibles restricts their ability to extract particles. Ants' pulling force has been measured to be 30-to-60 times their own weight [34]; for the ants studied herein $U \approx 3 - \text{to} - 6 \times 10^{-3}$N.

4.2.5 Comparison

Forces W, C, E and U are plotted in Fig. 5 for different values of the corresponding parameters. The particle self weight is greater than electrical attraction $W/E > 1$ for particle size d = 4-to-40 μm and greater than the capillary force $W/C > 1$ for size $d > 4$ mm. The ant pulling force U is enough to grab pellets of small particles, but only single gravel grains. These results highlight the importance of grain weight and capillary forces on ants digging behavior.

Capillary forces promote isotropic force distribution in moist silts and sands. This explains the construction of tunnels in all directions and the abundance of branches in wet soils. Ramps or tunnels at 30–40° may result from the optimization that combines both geomechanical stability with convenient transport (refer to Table 2). Likewise, isotropic

stability may explain the more convoluted nest geometries seen in lightly cemented soils (Liometopum apiculatum ants, [8]).

The maximum size of single grains and pellets is also limited by handling size restrictions (similar obervations with seeds, [35]), ants' strength and their ability to transport heavy grains without falling forwards (high overturning moment about their front legs). We observed that harvester ants experience equilibrium difficulties while transporting particles that are twice larger than their mandible size, $d/M \geq 2$ and $p/M \geq 2$; or in terms of forces when the pellet or particle weight to the ant weight is 3-to-4. Forward overturning is more prevalent in horizontal transport; in fact, ants transport bigger particles along vertical shafts by aligning the particle center of gravity with their bodies and distributing the weight among all legs.

4.3 Tunnel stability analysis

We investigate tunnel stability conditions using discrete element simulations for small tunnel-to-grain size D/d ratios (software EDEM v1.1—DEM Solutions) and an equivalent continuum solution for large D/d ratios.

4.3.1 Discrete element simulation

The 3D simulation consists of a cylindrical hopper filled with ~1,500 spherical particles and subjected to gravity discharge through a bottom orifice size D (Fig. 4c). Complimentary 2D simulations model a plane hopper with ~7,000 spherical particles. The discrete element simulation is extended to $\mathrm{D/d50} \approx 11 - 15$ in both 3D and 2D cases. The Hertz-Mindlin interparticle contact model is modified to incorporate a constant attractive force A to represent capillary C or electrical E forces at every interparticle contact in the granular mass. The size of particles d is Gaussian distributed with a standard deviation of $d_{50}/10$, in order to prevent the formation of regular packings. The inter-particle friction coefficient is set equal to $\mu = 0.5$. Simulations are repeated by varying the magnitude of the attractive force (C and/or E) until we find the minimum attractive force A when granular arches become unstable. Results show that the size of stable tunnels relative to the particle size D/d_{50} increases nonlinearly as the inter-particle attraction A increases (Fig. 6).

In the extreme case of dry particles with no attractive force, stable arches form when $D/d \leq 3.7$. This is in agreement with published experimental results gathered with various grains: granular arches form when D/d_{50} varies from 3.2-to-5 for smooth spherical glass beads, and when $D/d_{50} = 3.8$-to-5.2 for well rounded Ottawa sand [36]. These results explain the stability of tunnels in coarse gravel CG 6/10 ($D/d \sim 1.5$) and in fine gravel CG 10/14 ($D/d \sim$ 3.7) which remain open even after drying, and the need of capillary forces in fine grained soils.

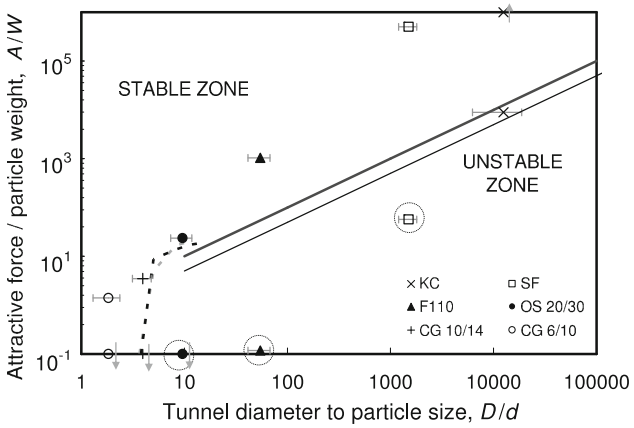

Fig. 6 Tunnel stability. Experimental observations (datapoints), numerical particle-level simulation (*dashed lines*) and limiting-equilibrium upper bound (*continuous line*). The vertical position of data points reflects the estimated range of capillary and electrical forces. Encircled data points correspond to intrinsically unstable tunnels where D/d is taken equal to its capillary-based value when tunnels are possible. *Arrows* indicate data points that are outside the scale. Gravels can sustain tunnels by grain arching in the absence of attractive forces when $D/d < 4$. All other soils require attractive forces to sustain stable tunnels

4.3.2 Equivalent continuum

The stability of tunnels at large D/d_{50} ratios is evaluated assuming an equivalent continuum with strength estimated from the interparticle attractive force as A/d^2. Then, limit equilibrium analysis permits computing the kinematically admissible upper bound solution for a failure mechanism that resembles a vertical cut in 2D and in 3D axisymmetric configurations (Fig. 4d),

$$\frac{A}{W} = \frac{6}{\alpha\pi}(1-n)\frac{D}{d} \tag{4}$$

where A/W is the minimum ratio of particle-level forces of attraction and self weight required for stability and n is the porosity of the packing. The geometric parameter α is equal to $\alpha = 1$ for 2D planar failure and $\alpha = 2$ for the 3D cylindrical model (Fig. 6, more rigorous solutions are found in [37,38]).

4.3.3 Comparison

All ant tunnels observed in our experiments plot on the stable zone in Fig. 6, above the boundaries found in the previous analyses. These results show the relevance of attractive forces on tunnel stability $D/d \geq 4$. The collapse of tunnels upon drying in silt SF ($D/d \sim 1,000$), sands F110 ($D/d \sim 35$)

and OS 20/30 ($D/d \sim 8$) add further validity to these predictions.

4.4 Excavation patterns

4.4.1 Excavation in fine grained sediments

The low digging rates in moist fine grained soils appear to reflect excavation difficulties at the tunnel face. The force required to pull a semi-spherical block of soil the size of the mandible M held by interparticle attraction forces A can be estimated as:

$$F = \frac{\pi}{4}\left(\frac{M}{d}\right)^2 A \tag{5}$$

We obtain the particle diameter d corresponding to the finest granular medium that ants can dig by equating this expression with the maximum pulling force $U \approx$ 3-to-6 $\times\ 10^{-3}$ N. The computed value is $d = 100\,\mu$m i.e. sands range. In fact, in order to dig the wet clay KC ($d_{50} = 0.4\,\mu$m) and silt SF ($d_{50} = 5\,\mu$m), ants are forced to extract blocks smaller than the mandible size M size and to form pellets before transportation. Branching is more prevalent in looser soils where the ant finds abundant, readily removable zones to continue excavating.

4.4.2 Excavation in coarse sediments

Ants work as particle-level stability sensors and prefer excavating in the direction of force chains, rather than crossing them which is inherently unstable. This is most clearly seen in gravelly soils where ants remove loose particles first and avoid load-bearing particles that are part of force chains in the granular skeleton (recall observations related to Fig. 4a).

Furthermore, a large pull force is required to remove a particle from a load bearing chain (Fig. 4b): for interparticle friction μ and overburden stress $\gamma_{soil} \cdot z$ at depth z, the required pulling force is

$$F = 2\gamma_{soil} z d^2 \mu \tag{6}$$

For example, for a pulling force $U = 5$ mN, friction $\mu = 0.50$ and depth $z = 0.1$m, the largest load-bearing particle an ant can extract is $d \approx 2$ mm. The increase in overburden stress with depth prevents the removal of load-bearing particles, and branching becomes less frequent with depth (observed in natural nests, refer to [11]). If the ant manages to pull a load bearing particle out of the granular chain, partial collapse follows until a new arch forms.

This analysis explains the prevalence of vertical shafts in coarse sediments as there are free particles at the base of shafts, but most particles tend to be load-bearing on tunnel walls. Ants' ability to sense particles does not necessarily avoid collapses: apparently, ants fail to recognize the role of "secondary particles" which are not part of load chains, but support global equilibrium by preventing chain buckling.

4.4.3 Excavation next to interfaces

The preferential excavation of soils near rigid vertical and horizontal interfaces both in coarse and fine grained soils (also noted in [27,39]) may reflect the following geomechanical causes: (1) grains pack looser against interfaces [40], (2) mechanical compliance leads to lower stress in the sediment near the interface, and (3) there is enhanced granular stability and fewer potential sliding blocks against rigid interfaces.

4.5 Saturation and tunnel flooding

Soils may remain saturated $S = 100\%$ above the water table (i.e., the upper bound for the hydrostatic condition) because air invasion into the soil is prevented by the tensile air–water interface membrane that adheres to boundary grains; conversely, the generated suction s prevents water from flowing out of the soil. Therefore, tunnels do not flood in sediments above the free water table under steady state conditions, regardless of their degree of saturation.

The "air entry value" defines the maximum water suction that may develop in a soil mass before air invasion, and it is inversely proportional to the pore size or the particle size. Capillary rise is an analogous, complementary measure of pore size. Given the low air entry value in coarse sands and gravels, the capillary rise is minimal, and sediment saturation is always associated to tunnel flooding in coarse grained sediments.

5 Summary: boundaries for ants digging behavior

Excavation at the tunnel face and grain transport are determined by: (1) the ants height H, mandible size M and pulling force U, (2) the soil grain size d or specific surface S_S, and (3) moisture conditions in terms of water content ω or degree of saturation S. The nest architecture at the macroscale evolves -in part- from these conditions at the tunnel face.

Geometric and force-balance relations define ants' digging behavior in soils, as summarized in Fig. 7. Salient geometric restrictions include: (1) minimum tunnel size to ant height to satisfy traffic needs $D/H \geq 2$, (2) single particle grabbing capability $d \leq M$, (3) stable tunnel size D for large size particles d in the absence of attractive forces $D/d \leq 4$. Ant geometric characteristics can be used to re-write these boundaries in terms of ant size, in particular, the ant height is about twice the mandible size $H \approx 2M$. Excavation and stability restrictions related to ant strength and particle-level forces include: (1) capillary force to the particle self weight

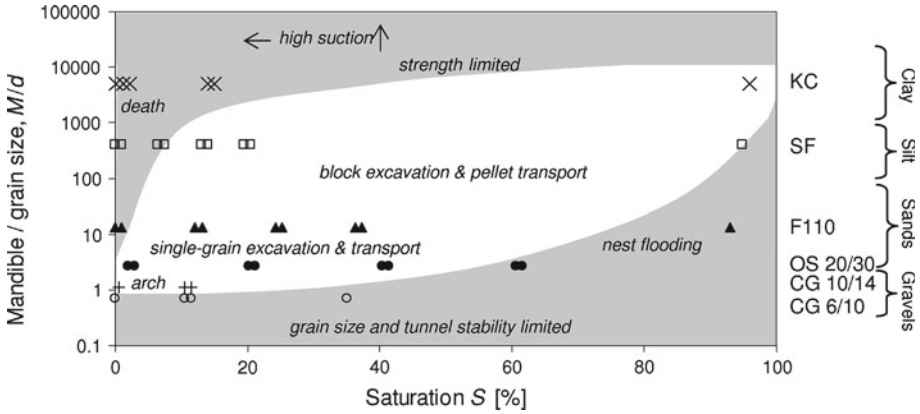

Fig. 7 Geometrical and geomechanical controls and restrictions on ants digging behavior and nest architecture

C/W, and (2) the ant pulling strength to the force required to extract a particle or a block U/F.

Within their inherent size and strength limitations, ants exhibit an exceptional ability to adapt excavation strategies, transport methods and nest architectures to the prevailing sediment (grain size, packing density) and geomechanical conditions (moisture, stress field, and boundary conditions). The excavation strategy mobilizes the internal strength in the granular medium, properly accounting for friction, suction and arching effects. The resulting tunnel structure emerges as a mechanically-convenient and energy-efficient topology based on local information gather by ants along the tunnel and at the tunnel face.

Acknowledgments Support for this research was provided by the Goizueta Foundation and the National Science Foundation.

References

1. Bugliarello, G.: Biomimesis: The Road Less Traveled. Bridge **27**(3) (1997)
2. Bonte, D. et al.: Microgeographical distribution of ants (Hymenoptera: Formicidae) in coastal dune grassland and their relation to the soil structure and vegetation. Anim. Biol. **53**(4), 367–377 (2003)
3. Kleineidam, C, Ernst, R., Roces, F.: Wind-induced ventilation of the giant nests of the leaf-cutting ant Atta vollenweideri. Naturwissenschaften **88**(7), 301–305 (2001)
4. Cox, M.D., Blanchard, G.B.: Gaseous templates in ant nests. J. Theor. Biol. **204**(2), 223–238 (2000)
5. Johnson, R.A.: Biogeography and community structure of north of North American seed-harvester ants. Ann. Rev. Entomol. **46**(1), 1 (2001)
6. MacMahon, J.A., Mull, J.F., Crist, T.O.: Harvester ants (Pogonomyrmex spp.): their community and ecosystem influences. Ann. Rev. Ecol. Syst. **31**, 265 (2000)
7. Wagner, D., Jones, J.B., Gordon, D.M.: Development of harvester ant colonies alters soil chemistry. Soil Biol. Biochem. **36**(5), 797–804 (2004)
8. Gregg, R.E.: The nest of the liometopum apiculatum mayr hymenoptera: formicidae. Univ. Colo. Stud. Ser. Biol. **11**, 1–6 (1963)
9. Nagel, H.G.: Western harvester ants in Kansas : Colony founding, nest structure and function, factors affecting density, and effect on soil formation—Ph.D. Thesis. In: Department of Entomology, pp. 180. Kansas State University, Manhattan Kansas (1969)
10. Johnson, R.A.: Habitat segregation based on soil texture and body size in the seed-harvester ants Pogonomyrmex rugosus and P. barbatus. Ecol. Entomol. **25**(4), 403–412 (2000)
11. Tschinkel, W.R.: The nest architecture of the Florida harvester ant, Pogonomyrmex badius. J. Insect Sci. **4**(21), 1–19 (2004)
12. Tschinkel, W.R.: The nest architecture of the ant, camponotus socius. J. Insect Sci. **5**(9), 18 (2005)
13. Wheeler, W.M.: Ants; their structure, development and behavior. pp. 663 Columbia University Press, New York (1910)
14. Buhl, J. et al.: Self-organized digging activity in ant colonies. Behav. Ecol. Sociobiol. **58**(1), 9–17 (2005)
15. Gladin, J.R.: Soil structure modification and nest disruption of red harvester ants, Pogonomyrmex barbatus, pp. 62. F. Smith—M.S. Thesis, Oklahoma State University (1983)
16. Clemencet, J., Doums, C.: Habitat-related microgeographic variation of worker size and colony size in the ant Cataglyphis cursor. Oecologia **152**(2), 211–218 (2007)
17. Wheeler, G.C., Wheeler, J.: The Ants of North Dakota. Dakota Press, Grand Forks, North Dakota (1963)
18. Cole, A.C.J.: The relation of the ant, Pogonomyrmex occidentalis CR., to its habitat. Ohio J. Sci. **32**, 133–146 (1932)
19. Aleksiev, A.S., Sendova-Franks, A.B., Franks, N.R.: The selection of building material for wall construction by ants. Anim. Behav. **73**(5), 779–788 (2007)
20. Wagner, D., Brown, M.J.F., Gordon, D.M.: Harvester ant nests, soil biota and soil chemistry. Oecologia **112**(2), 232–236 (1997)
21. Wheeler, W.M.: Notes on the marriage flights of some Sonoran ants. Psyche **24**, 177–180 (1917)
22. Kloft, W.J. et al.: Formica integra (Hymnoptera: Formicidae) 1. Habitat, nest construction, polygyny, and biometry. Fla. Entomol. **56**(2), 67–76 (1973)
23. Bollazzi, M., Kronenbitter, J., Roces, F.: Soil temperature, digging behaviour, and the adaptive value of nest depth in South American species of Acromyrmex leaf-cutting ants. Oecologia **158**(1), 165–175 (2008)
24. Moreira, A.A. et al.: External and internal structure of Atta bisphaerica Forel (Hymenoptera: Formicidae) nests. J. Appl. Entomol. **128**(3), 204–211 (2004)
25. Mikheyev, A., Tschinkel, W.: Nest architecture of the ant Formica pallidefulva: structure, costs and rules of excavation. Insectes Soc. **51**(1), 6 (2004)
26. Sudd, J.H.: The excavation of soil by ants. Z Tierpsyschol **26**, 257–276 (1969)
27. Sudd, J.H.: Specific patterns of excavation in isolated ants. Insectes Soc. **17**, 253–260 (1970)

28. Hooper-Bui, L.M., Appel, A.G., Rust, M.K.: Preference of food particle size among several urban ant species. J. Econ. Entomol. **95**(6), 1222–1228 (2002)
29. Jungerius, P.D., van den Ancker, J.A.M., Mucher, H.J.: The contribution of termites to the microgranular structure of soils on the Uasin Gishu Plateau, Kenya. Catena **34**(3–4), 349–363 (1999)
30. Lavelle, P.: Faunal activities and soil processes: Adaptive strategies that determine ecosystem function. In: Proc. 15th World Congress of Soil Science. Acapulco, Mexico (1994)
31. Zou, R.P. et al.: Coordination number of ternary mixtures of spheres. Part. Part. Syst. Characterization **20**(5), 335–341 (2003)
32. Cho, G.C., Santamarina, J.C.: Unsaturated particulate materials—particle-level studies. J. Geotech. Geoenviron. Eng. **127**(1), 84 (2001)
33. Santamarina, J.C., Klein, K.A., Fam, M.A.: Soils and Waves. pp. 488 J. Wiley and Sons, Chichester, England, New York (2001)
34. Sudd, J.H.: Transport of prey by ants. Behaviour **25**, 234–271 (1965)
35. Gomez, C., Espadaler, X., Bas, J.M.: Ant behaviour and seed morphology: A missing link of myrmecochory. Oecologia **146**(2), 244–246 (2005)
36. Valdes, J.R., Santamarina, J.C.: Particle clogging in radial flow: Microscale mechanisms. SPE J. Richardson **11**(2), 193–198 (2006)
37. Davis, E.H. et al.: The stability of shallow tunnels and underground openings in cohesive material. Geotechnique **30**(4), 397–416 (1980)
38. Terzaghi, K.: Rock defects and loads in tunnel support. In: Proctor, R.V., White, T. (eds.) Rock Tunneling with Steel Supports, pp. 15–99. Commercial Shering Co., Youngstown, Ohio (1946)
39. Sudd, J.H.: The response of isolated digging worker ants [Formica lemani and Lasisus niger] to tunnels. Insectes Soc. **17**, 261–271 (1970)
40. Graton, L.C., Fraser, H.J.: Systematic packing of spheres with particular relation to porosity and permeability. J. Geol. **43**(8), 785–909 (1935)